Spectral analysis of Enceladus, Dione, and Rhea' surfaces: water ice and sub-micron particles distribution. F. Scipioni[1], P. Schenk[2], F. Tosi[3], E. D'Aversa[3], R. Clark[4], D. P. Cruikshank[1], J.-Ph. Combe[5], C. Dalle Ore[6]. [1]NASA Ames Research Center, Moffett Field, CA, 94035, francesca.scipioni@nasa.gov; [2]Lunar and Planetary Institute; [3]INAF-IAPS, Rome, Italy; [4]PSI, Tucson, AZ; [5]Bear Fight Institute, Winthrop, WA; [6]Seti Institute, Mountain View, CA.

Water ice is the most abundant component of Saturn's mid-sized moons. However, these moons show an albedo asymmetry – their leading sides are bright while their trailing side exhibits dark terrains. Such differences arise from two surface alteration processes.

The first is due to bombardment of charged particles from the interplanetary medium and driven by Saturn's magnetosphere (e.g. [1]). These particles fracture the surface, forming sub-micron ice particles, and get contaminants implanted in the upper ice layer (e.g. [2]). The second process results from the impact of E-ring particles on the satellites' leading side. The E-ring is composed primarily of pure water ice grains, which originate from Enceladus' southern polar plumes. Tethys, Dione, and Rhea orbit outside the E-ring, while Mimas orbits inside. E-ring ice particles are continuously refreshing the leading hemisphere surfaces of Tethys, Dione, and Rhea, thereby making them bright (e.g. [3] [4] [5] [6] [7] [8]).

We present here results from our ongoing work mapping the variation of the main water ice absorption bands and sub-micron ice particles across Dione, Rhea, and Enceladus' surfaces using Cassini-VIMS data acquired in the IR range (0.8–5.1 μm).

The Cassini VIMS spectrometer acquires hyperspectral data in the 0.3–5.1 μm spectral range. We selected VIMS cubes of Enceladus, Dione, and Rhea in the IR range (0.8–5.1 μm), and minimized photometric effects due to different illumination conditions by normalizing all spectra at 2.23 μm.

For all pixels in the selected VIMS cubes, we measured the band depths for water-ice absorptions at 1.25, 1.5 and 2.02 μm and the height of the 3.6 μm reflection peak, whose value relates to grain size.

Moreover, we considered the main spectral indictors in the IR range for ice particles smaller than 1 μm [9]: (i) the 2 μm absorption band is asymmetric and (ii) it has the minimum shifted to longer λ; (iii) the band depths ratio 1.5/2.0 μm decreases; (iv) the reflection peak at 2.6 μm decreases; (v) the Fresnel reflection peak is suppressed; (vi) the 5 μm reflectance is decreased relative to the 3.6 μm peak.

Since the first part of the VIMS-IR spectra (0.8-2.5 μm) is sometimes affected by saturation effects, for each cube of the dataset we performed a pixel by pixel selection of spectral features to be used: for each pixel, only the absorption bands not suppressed (totally or partially) by saturation were selected.

To characterize the global variation of water-ice band depths we sampled the three satellites' surface with a 1°x1° fixed-resolution grid and then averaged the band depths and peak values inside each square cell.

In Figure 1 we show the global variation of the water ice absorption band, centered at 2.02 μm, and in Figure 2 the variation of band depths ratio 1.5/2.0 μm, for Enceladus (panel a), Dione (panel b), and Rhea (panel c).

The variation of the depth of the water ice absorption bands across the surface reflects the different space weather mechanisms acting on their surface. Terrains where E-ring's ice particles deposit have in general deeper water ice absorption bands, meaning that mechanism refreshes that portion of surface. On the other hand, terrains subject just to bombardment of charged particles and micrometeorite gardening have shallower absorption bands. This can be due to an increase in contaminants abundance, and/or to a finer grain size.

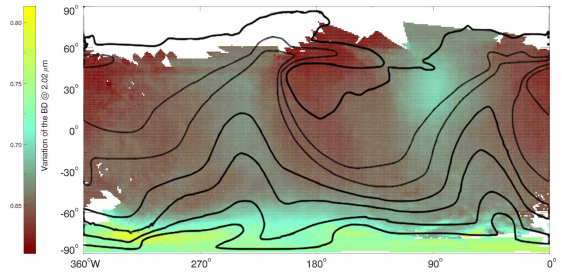

(a)

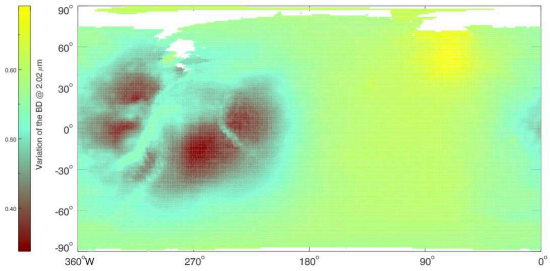

(b)

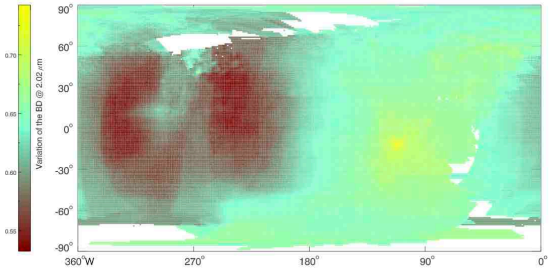

(c)

Figure 1: Variation of the water ice absorption band at 2.02 µm for Enceladus (a), Dione (b), and Rhea (c).

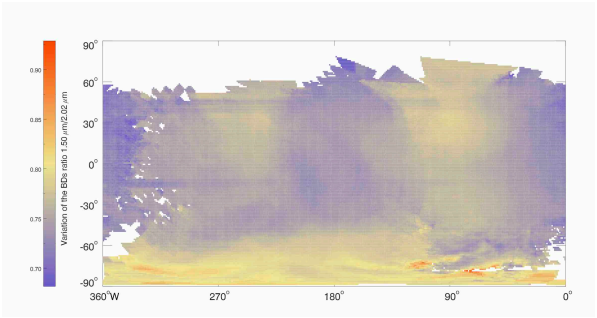

(a)

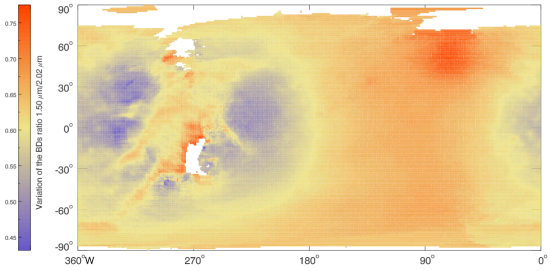

(b)

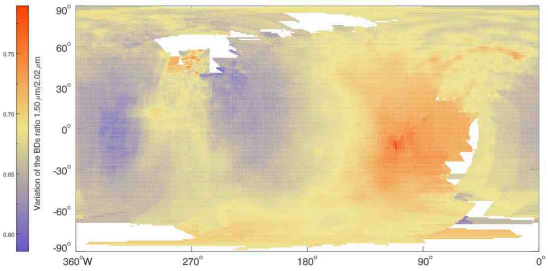

(c)

Figure 2: Variation of the band depths ratio 1.5/2.0 µm for Enceladus (a), Dione (b), and Rhea (c).

References:

[1] Schenk, P., et al., 2011. Icarus 211, 740–757. [2] Baragiola, R. A., et al., 2013. In: Gudipati, M. S., Castillo-Rogez, J. (Eds.), Vol. 356, p. 527. [3] McCord, et al., 1971. Astrophys. J. 165, 413–424. [4] Blair, G., Owen, F., 1974. Icarus 22, 224–229. [5] Buratti, et al., 1990. Icarus 87, 339-357. [6] Verbiscer, A.J. and Veverka, J., 1992. Icarus 99, 63-69. [7] Scipioni, F., et al., 2013. Icarus 226, 1331-1349. [8] Scipioni, et al., 2014. Icarus 243, 1-16. [9] Clark, R., et al., 2012. Icarus 218, 831-860.